Vibration measurements of the beamtube: bare tube, new trial insulation, initial insulation

John Worden, Peter Fritschel and Rainer Weiss June 3, 2014

Introduction Measurements of the beamtube vibrations were made of the newly insulated section of tube. These were compared with a bare section of tube and, where there was useful prior data, with the original insulated tube. The new insulation was 3 inch thick R10 insulation compressed to the 1 ¾ inch height of the tube stiffening rings. The outer jacket was a 16 mil thick composite aluminum layer impervious to rodents. The original insulation was a double layer. The one closest to the tube was 4 inch thick fiberglass (high temperature 1000F Knauf ductwrap) covered by aluminum foil and a second layer 2 inches thick fiberglass (lower temperature 250F Knauf ductwrap) with a final aluminum foil radiation shield. The original insulation was permeable by rodents.

The measurements were made with Wilcoxin Model 731A/P31 accelerometers. One accelerometer was placed on the enclosure floor and a second in the middle of the tube at a stiffening ring or on a support ring at the bellows between tube sections. The sound field in the enclosure was measured with a Radio Shack sound level meter. The amplitude of the transfer function between ground motion and tube motion as well as that of the sound field and tube motion are the principal results of the measurement. They show that below 25Hz the primary source of motion of the tube is ground motion while above 100 Hz it is acoustic. Below 25Hz the bare tube, and the new and old insulated tube have comparable transfer functions. In the band around 50Hz, the mixed inertial and acoustic region, the motion of the tube is smallest with the original insulation, a factor of 2 to 5 larger with the new insulation and a factor of 10 to 20 larger still for the bare tube. In the acoustic driven regime above 100Hz the motion of the tube is again smallest with the old insulation about a factor of 10 larger for the new insulation and a factor 100 larger for the bare tube. The actual spectra are shown in figures in the report.

The motion of the tube is smaller in the longitudinal direction (the direction along the tube axis), the one the interferometer is most vulnerable to for phase noise from scattered light from the baffles. The radial motion can be 5 to 10 times larger. The radial motions are more easily driven by sound than the longitudinal motions. The most prominent resonance of the tube is at about 14Hz in a mode transverse to the tube axis. This mode is primarily driven by ground noise.

Data

Table 1 Insulation parameters

Material	density kg/m^3	thickness m	thermal k w/Km	sound absorption db @100Hz	max temperature
new insulation 202-96 R10	1.03×10^{-5}	8.6×10^{-2}	0.048	1	123C insul 116C jacket
old Knauf ductwrap HT	2.6×10^{-5}	1.06×10^{-1}	0.035	2-3	500C
old Knauf ductwrap LT	1.12×10^{-5}	5.1×10^{-2}	0.040	1	120C

Table 2 Masses

Component	mass in kg/19 meter section
Stainless steel tube	1910
stiffening rings	165
new insulation	58
new jacket	92
old insulation	238

The difference between the transfer function for acoustic excitation of the tube between the new and old insulation is most likely attributable to the difference in the construction of the insulating layer The mass of the new insulation is about ½ of the old insulation which accounts for some of the increased acoustic sensitivity. More significant is that the aluminum jacket of the new insulation is in direct contact with the stiffening rings which most likely increases the sound conduction to the tube and would also increase the thermal coupling. If we go with this insulation we should consider an insulating layer between the jacket and the stiffening rings.

Some evidence for this comes from applying the acoustic pressure spectrum (**Figure 17**) to the tube and comparing the result with the radial acceleration (**Figure 16,19**). At high acoustic frequencies (above 100 Hz) when the acoustic wavelength $\lambda < 2\pi a$, where a is the tube radius, the acceleration spectrum of the tube becomes $a(f) = \frac{p(f)}{\sigma}$ where p(f) is the acoustic pressure spectrum and σ is the total tube mass /area. At lower frequencies (below 80Hz) the acceleration spectrum becomes smaller due to sound diffraction around the tube and varies as $a(f) = \frac{2\pi a f p(f)}{\sigma c_{sound}}$.

The actual displacement of the beamtube on a stiffening ring for both the bare and new insulated tube is shown in **Figure 1** (longitudinal motion) and **Figure 2** (radial motion) . (An earlier version of this report had an error in the accelerometer gain of a factor of 100)

It would be good to establish the ability of the new insulation to withstand a 150C bake in the event that we need to once again bakeout the tube. This could be done by adding a second layer to the existing new insulation to get comparable thermal conductivities to the original insulation.

Figure 20 shows estimates for the displacement noise due to scattering by the baffles when driven by the seismic and acoustic noise. The actual calculations are shown in LIGO T1300354-v3 by P. Fritschel and H. Yamamoto who estimate the scattering from the test mass non-uniform coatings. Given the large variability in the environmental conditions at the LIGO sites and the uncertainties in the scattering calculations, the margin between the equivalent displacement noise from the scattering and the advanced LIGO displacement sensitivity is not large enough to be comfortable. The acoustic sensitivity of the beamtube covered with the new insulation needs to be reduced.

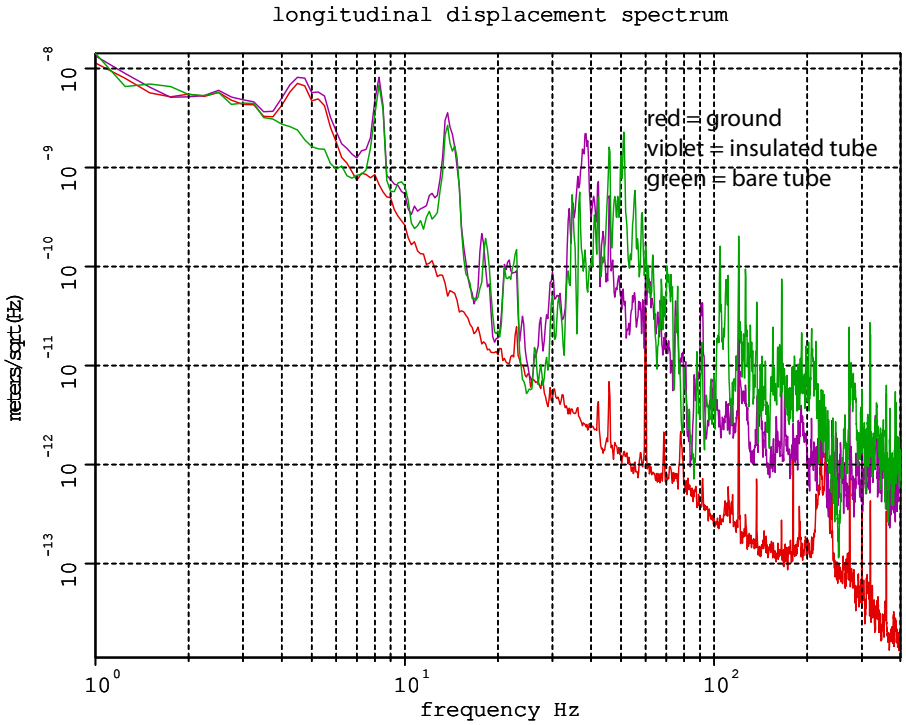

Figure 1 Longitudinal (along the tube axis) displacement spectrum. The accelerometer was mounted on a stiffening ring near the center of the tube section. The ground and acoustic noise in the enclosure was the driving source. The data between 4 and 6 Hz is affected by the change in seismic noise between measurements.

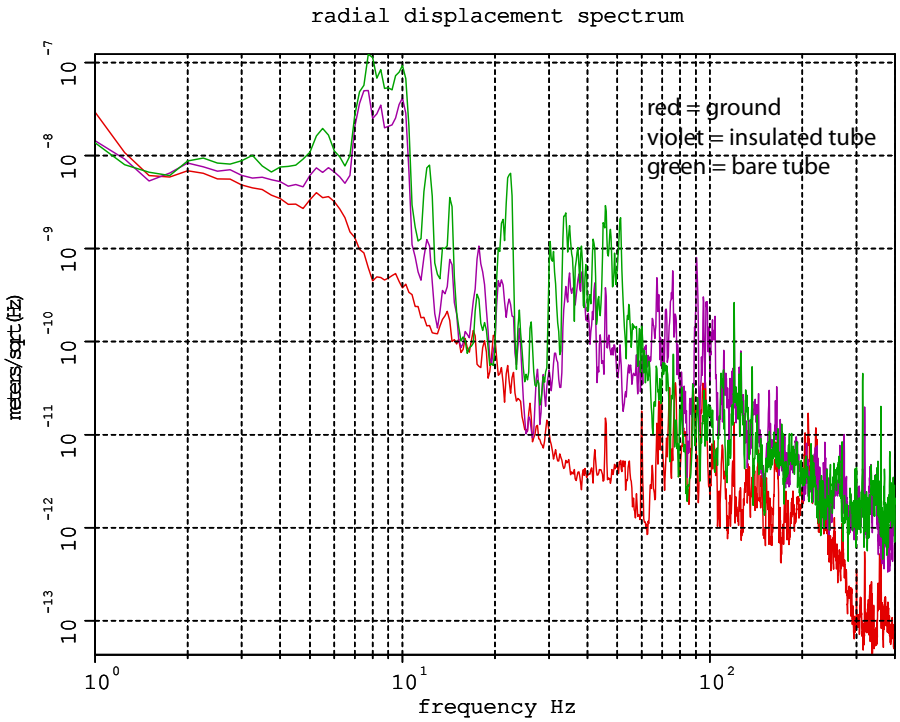

Figure 2 Radial displacement noise (perpendicular to the tube axis). The accelerometer was mounted on a stiffening ring near the center of the tube section.

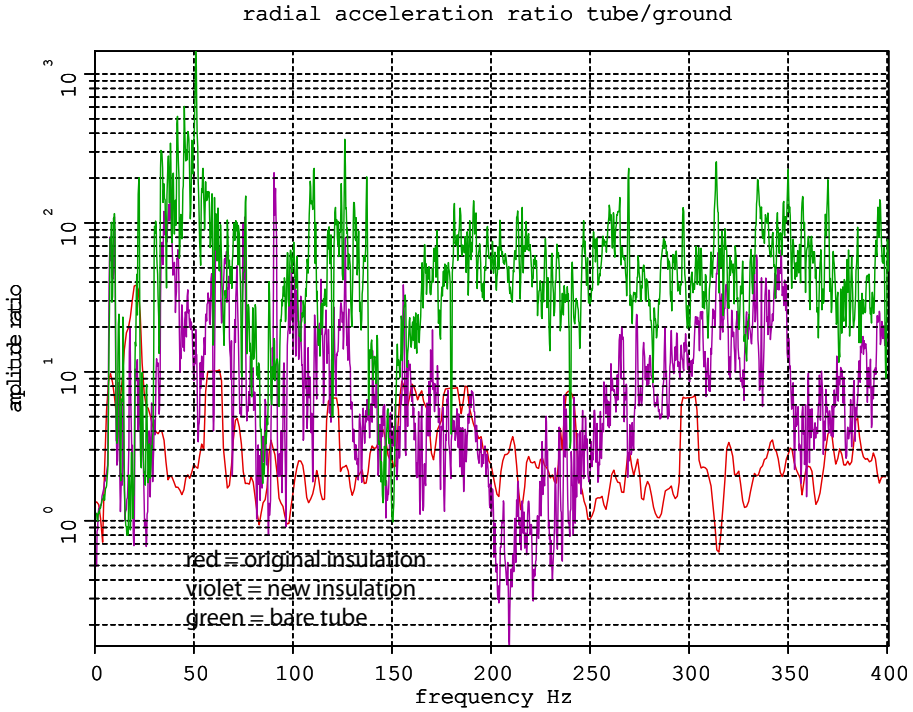

Figure 3 Full bandwidth spectrum of the ratio of the horizontal transverse motion of the tube divided by that of the enclosure floor. The motion includes both inertial and acoustic components. The old data includes significant 60Hz and harmonics from vibration of local transformers.

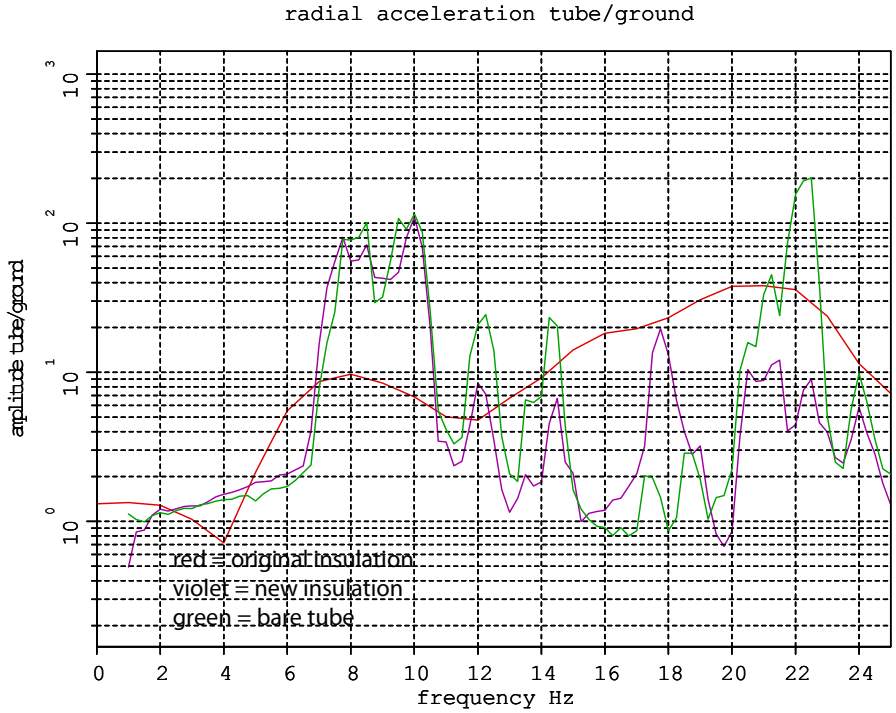

Figure 4 Same data as **Figure 3** expanded to low frequency. The resolution of the new data is ¼ Hz while the original insulation data was 1.5 Hz

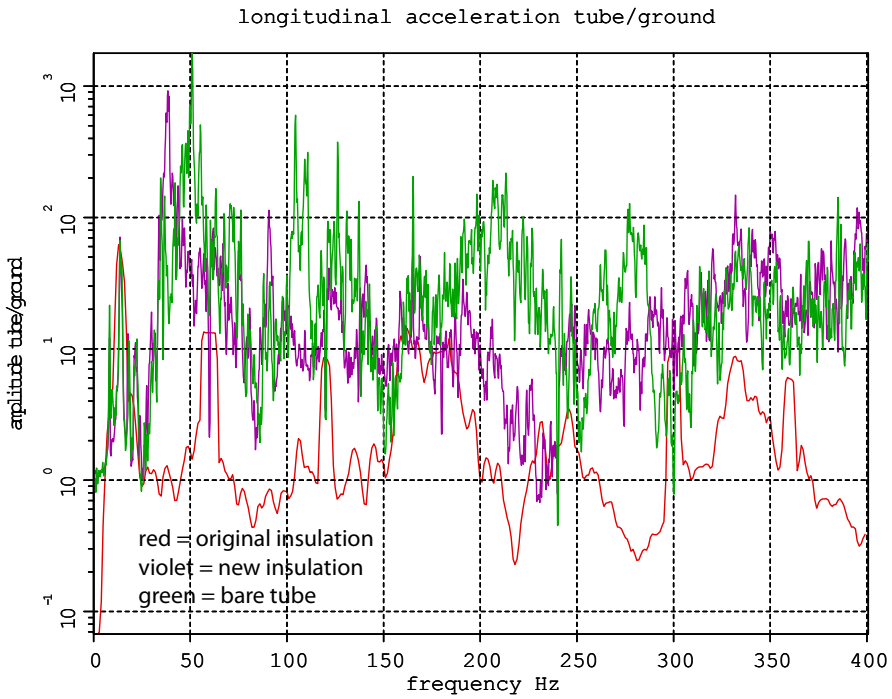

Figure 5 Full bandwidth spectrum of the ratio of the horizontal longitudinal motion of the tube divided by that of the enclosure floor. The motion includes both inertial and acoustic components.

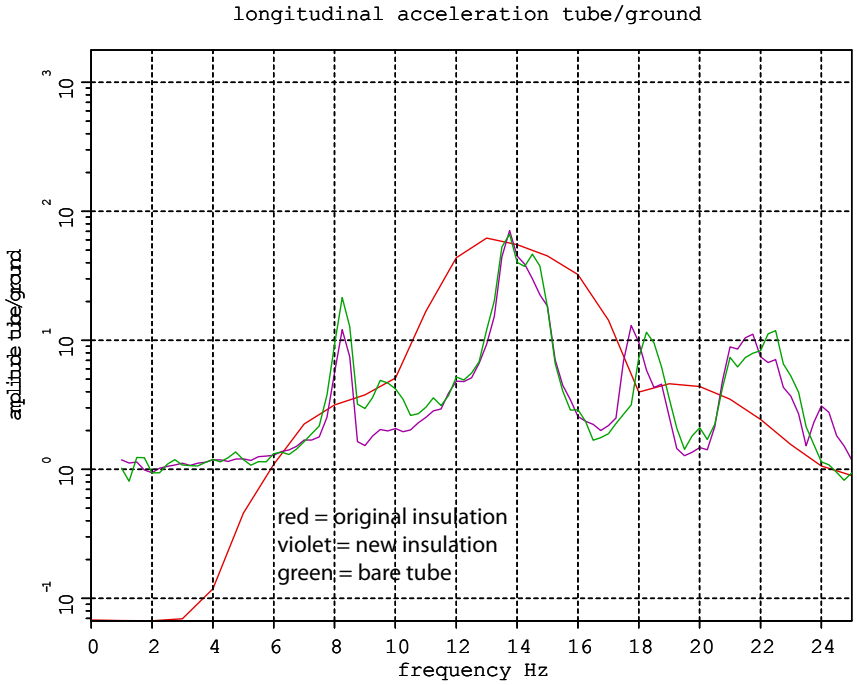

Figure 6 Same data as **Figure 5** expanded to low frequency. The resolution of the new data is ¼ Hz while the original insulation data was 1.5Hz. The spectrum shows the dominant mode at 14 Hz.

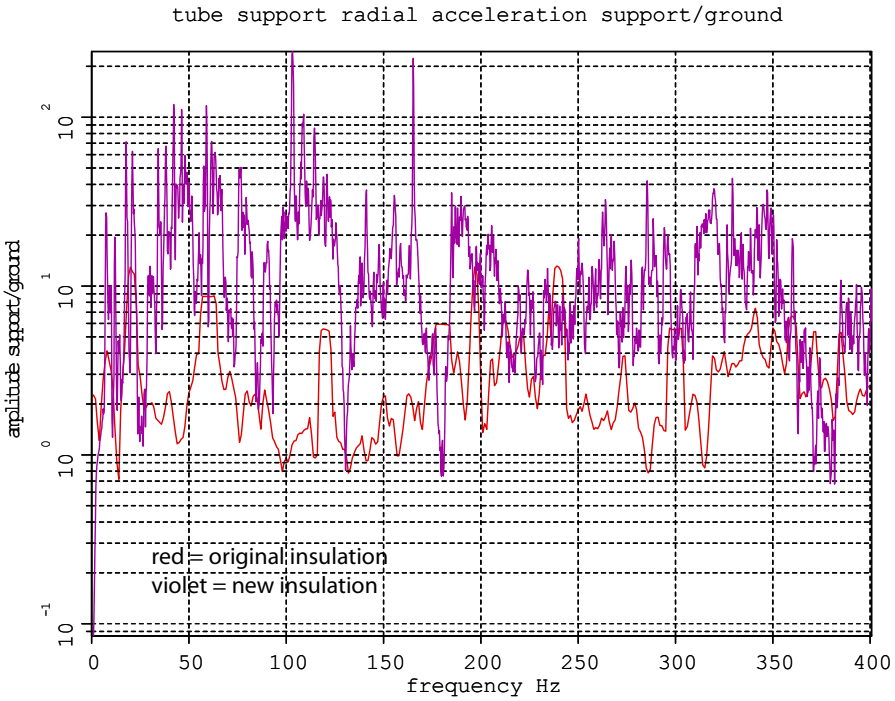

Figure 7 Full bandwidth spectrum of the ratio of the horizontal radial motion of the support ring at the bellows of the old and new insulated tubes to the motion on the ground.

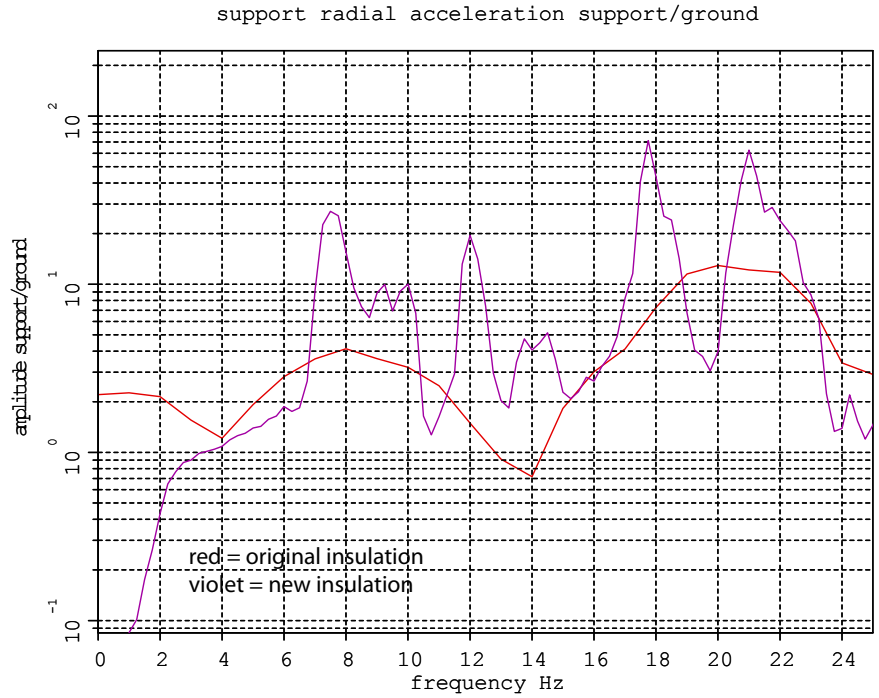

Figure 8 Same data as **Figure 7** expanded to low frequency. The resolution of the new data is ¼ Hz while the original insulation data was 1.5 Hz.

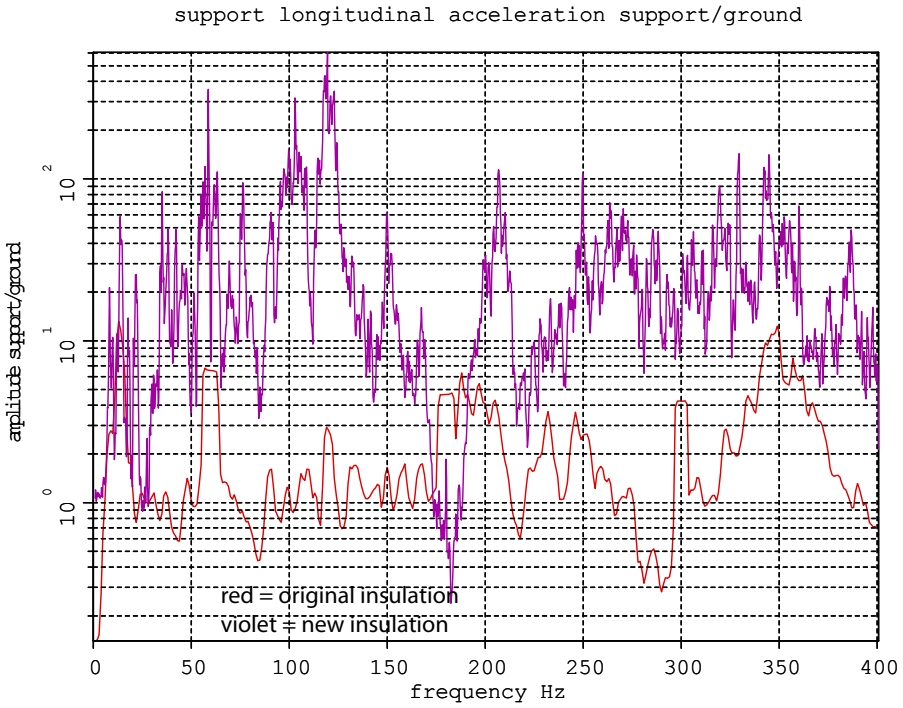

Figure 9 Full bandwidth spectrum of the ratio of the horizontal longitudinal motion of the support ring at the bellows of the old and new insulated tubes to the motion on the ground.

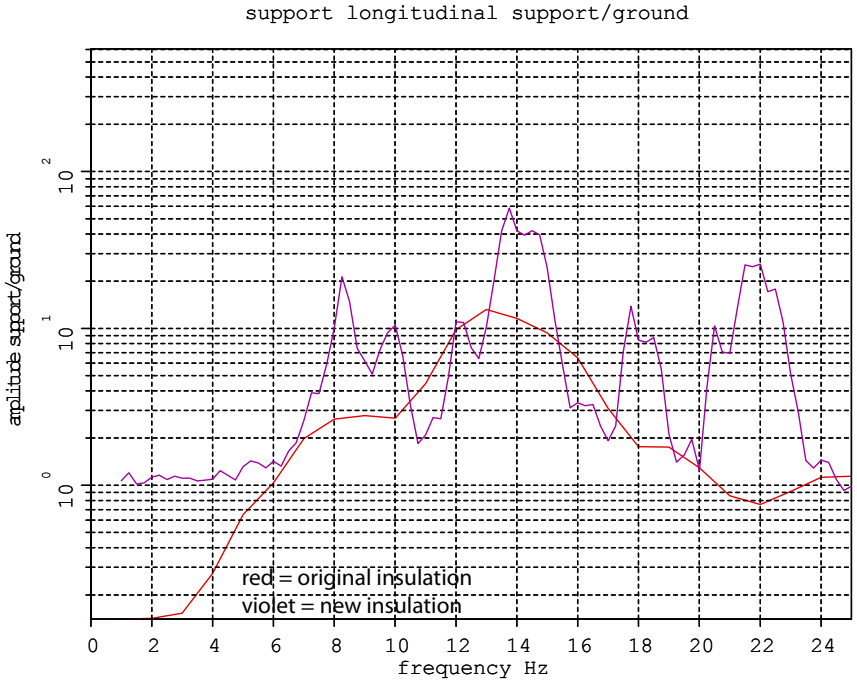

Figure 10 Same data as **Figure 9** expanded to low frequency. The resolution of the new data is ¼ Hz while the original insulation data was 1.5 Hz.

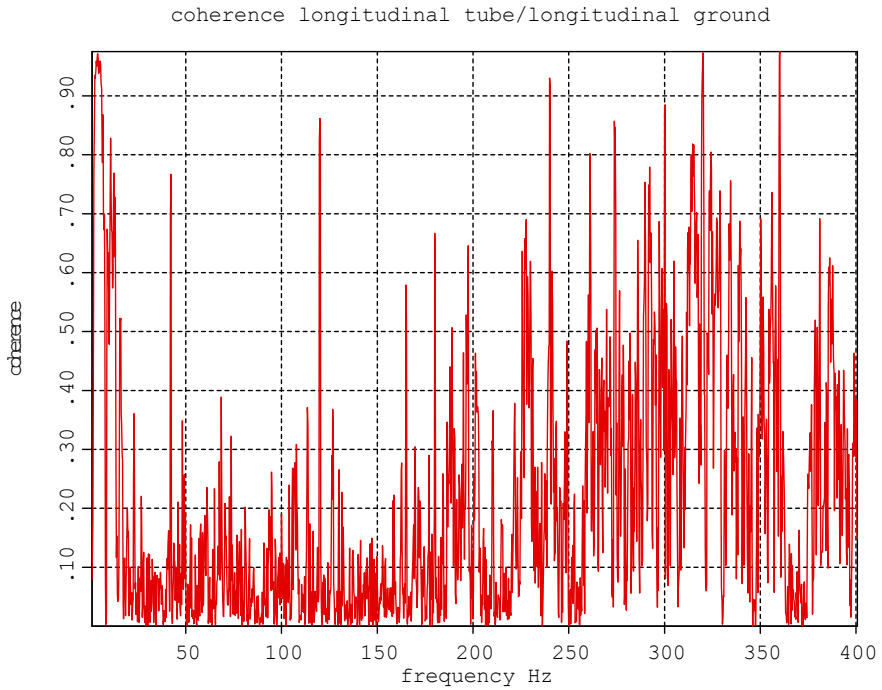

Figure 11 Coherence between accelerometer on the stiffening ring of the tube with the accelerometer on the ground both along the longitudinal direction.

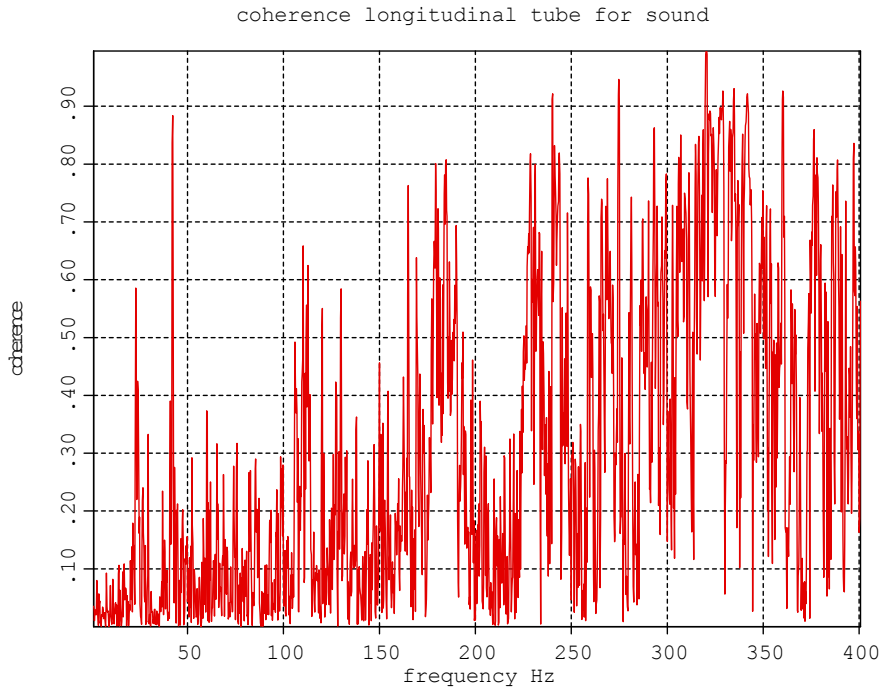

Figure 12 Coherence between the accelerometer on the stiffening ring of the tube and the sound meter in the enclosure.

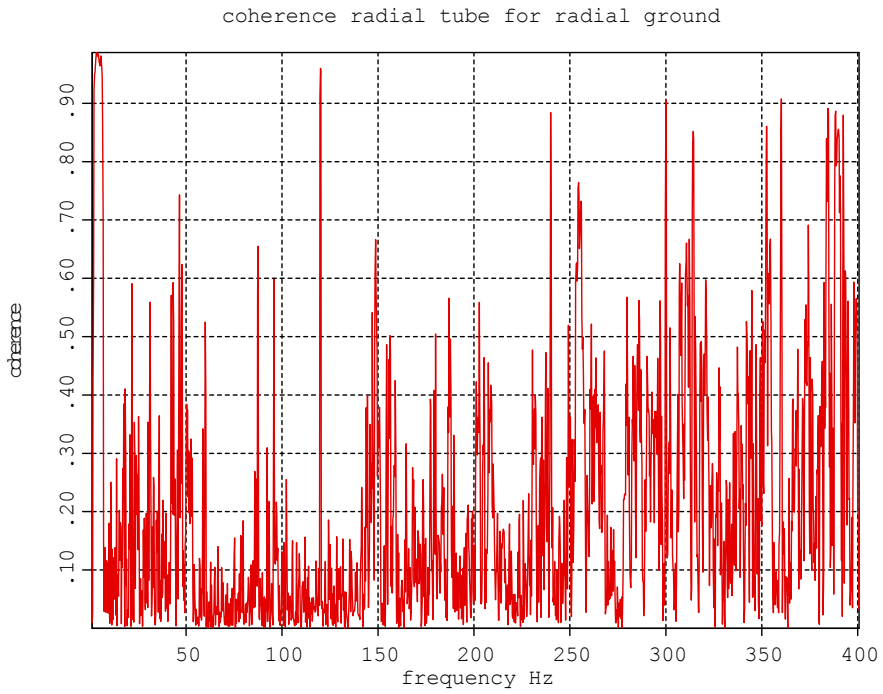

Figure 13 Coherence between the accelerometer on the stiffening ring on the tube and one on the ground both in the horizontal radial direction.

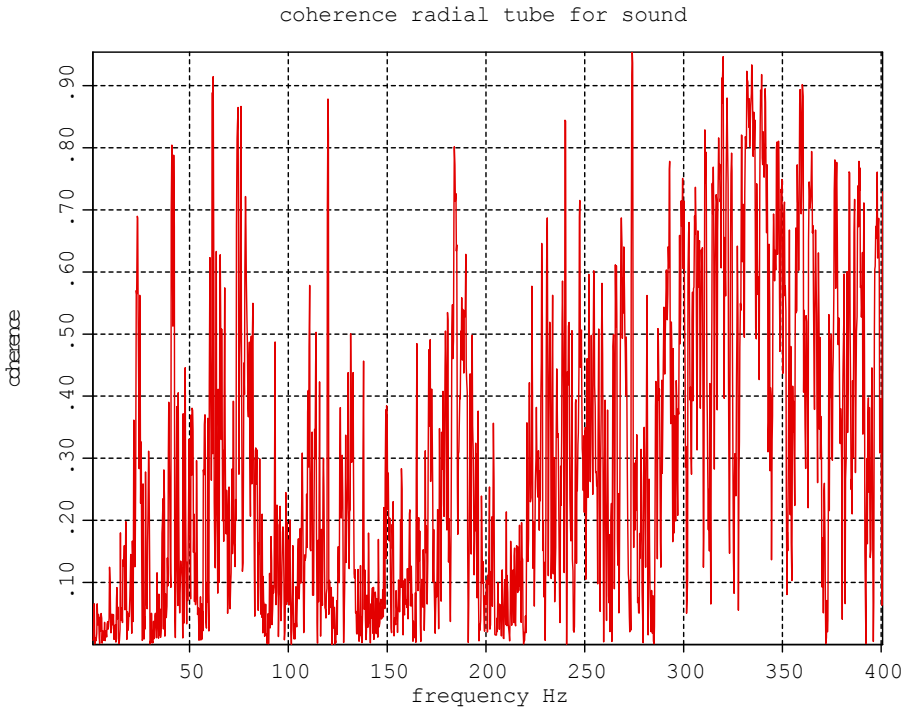

Figure 14 Coherence between the accelerometer on the stiffening ring on the tube and the sound meter in the enclosure.

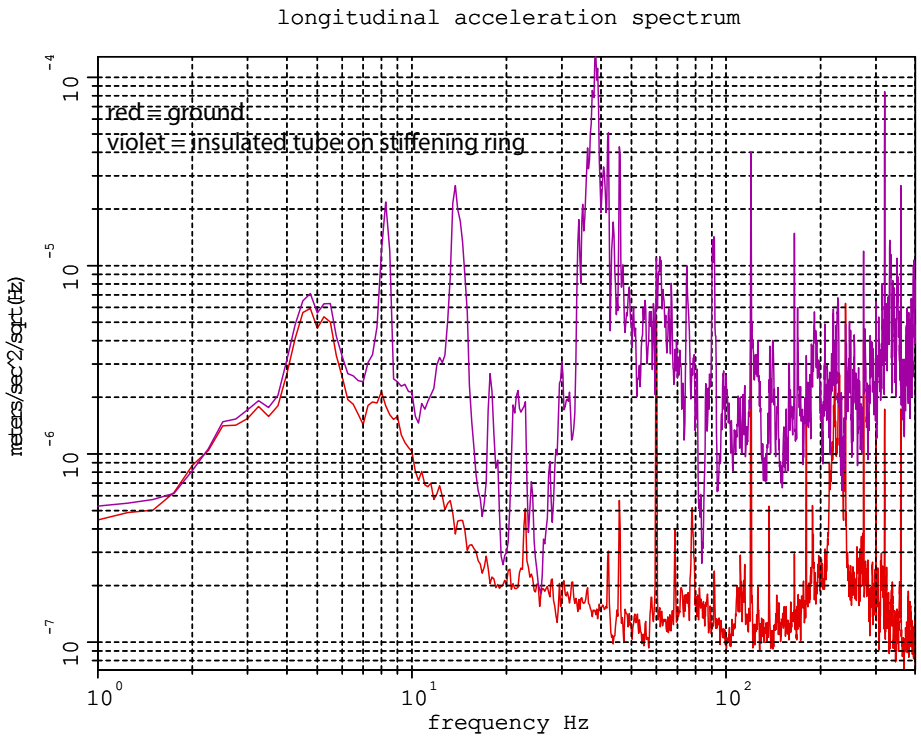

Figure 15 The longitudinal acceleration spectrum on the ground and the stiffening ring at the center of the insulated tube.

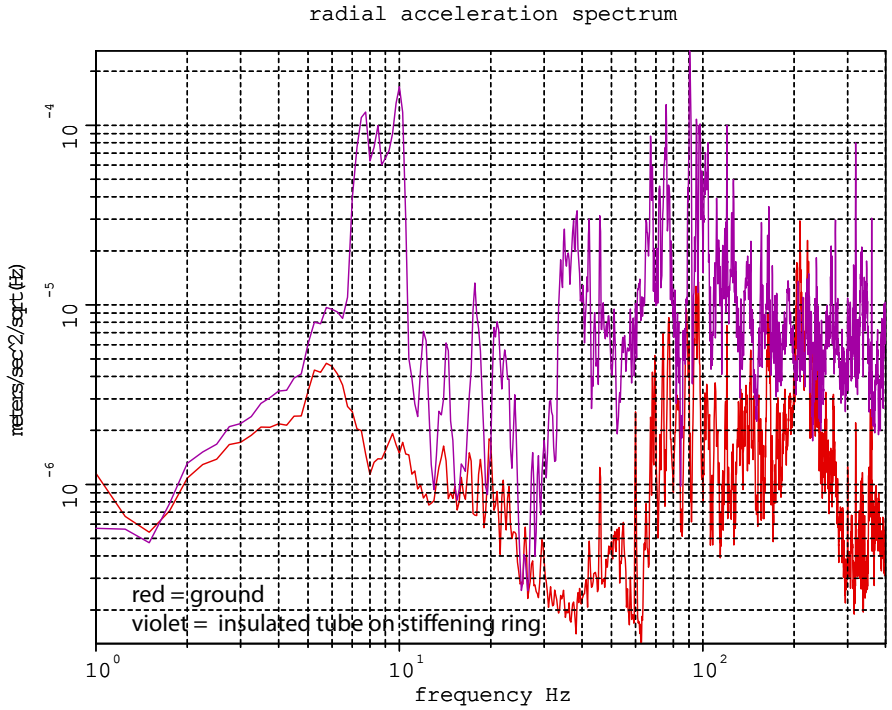

Figure 16 The radial acceleration spectrum on the ground and the stiffening ring at the center of the insulated tube.

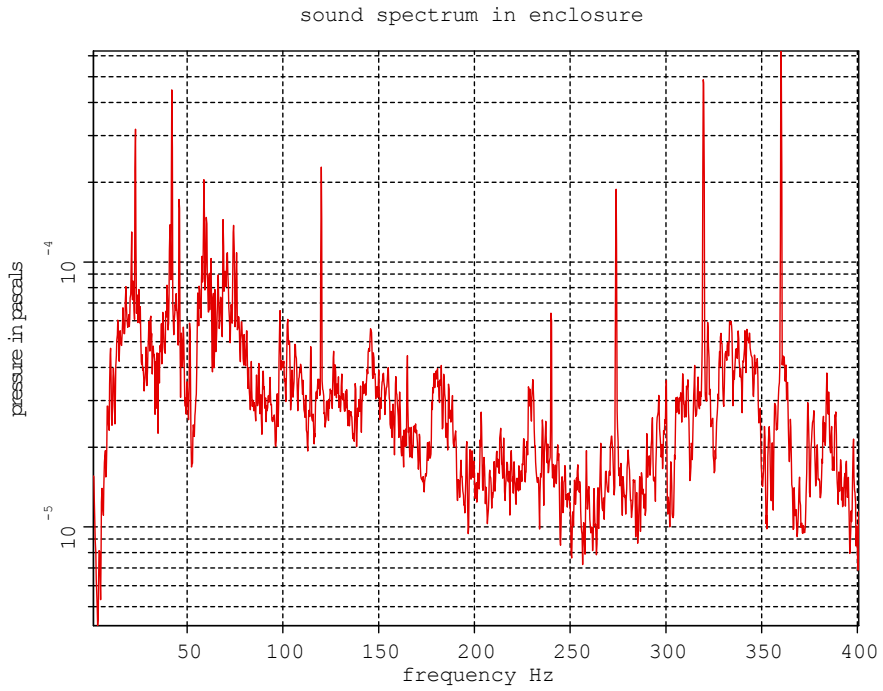

Figure 17 Sound pressure spectrum measured in the enclosure. The peaks at multiples of 30Hz come from a fan in the spectrum analyser.

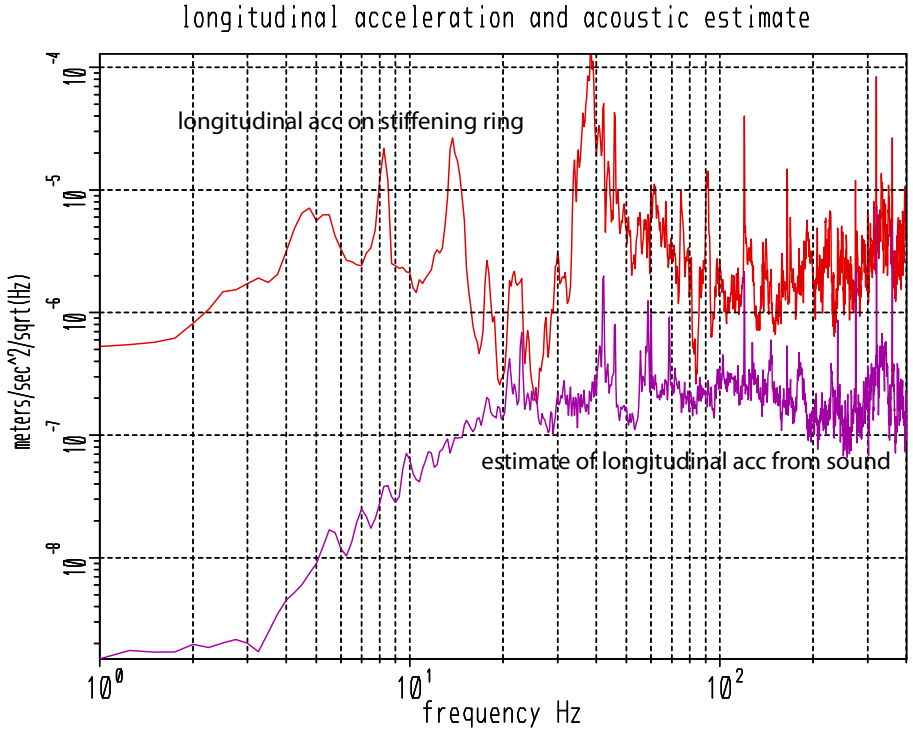

Figure 18 The longitudinal acceleration spectrum measured on a stiffening ring near the center of the tube insulated tube section. The spectrum as estimated from the sound pressure spectrum using 80Hz as the separation between the direct and the diffraction region with a mass per area of the tube of 97kg/m^2. The agreement is better than it looks as the tube is filled with resonances

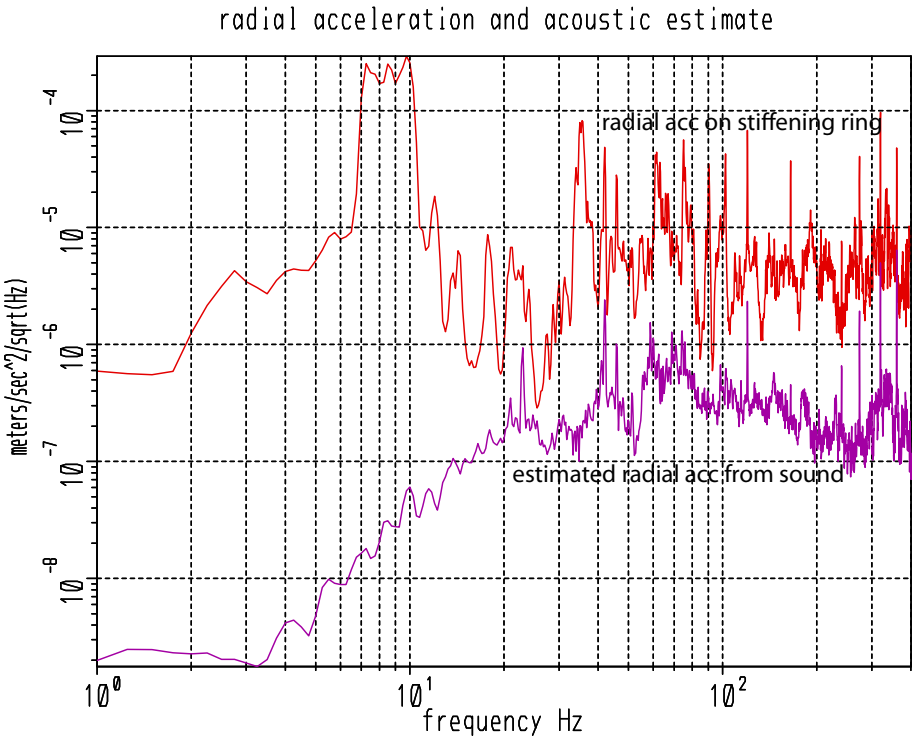

Figure 19 Similar to **Figure 18** for the radial acceleration spectrum.

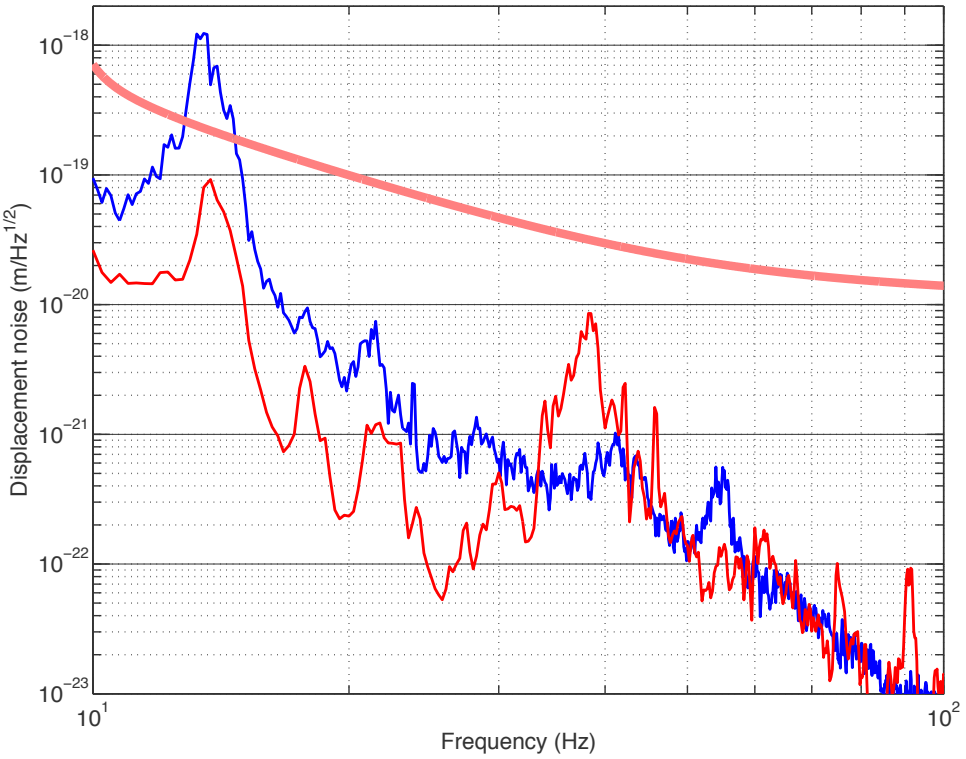

Figure 20 Displacement noise due to scattered light recombination from the beamtube baffles estimated for the test mass mirrors with the non-uniform coatings. The blue curve is the same as in **Figure 11** of document LIGO T1300354-v3 using beamtube motions measured by Robert Schofield during winds at LHO between 20 and 30 mph. In those measurements the beamtube was covered with the old insulation and was less sensitive to acoustic excitations than the newly insulated tube. Red curve is from the data in this report with the new insulation under conditions of low wind. The smooth red curve is the GWINC estimate for the advanced LIGO interferometer sensitivity with 125W input. We do not consider the margin between the estimated scattering noise and the desired advanced LIGO sensitivity large enough. The environmental conditions at the site vary by factors of 30 and the scattering calculations could well be too optimistic by factors of 10 or more .